*Polish Journal of Chemical Technology, 19, **4**, 59—64, 10.1515/pjct-2017-0068*

Adsorption of propan-1-ol vapour on Sorbonorit 4 activated carbon – equilibrium and dynamic studies

Dorota Downarowicz, Katarzyna Ziętarska*

West Pomeranian University of Technology, Szczecin, Department of Chemical Engineering and Environmental Protection Process, al. Piastow 42, 71-065 Szczecin, Poland
**Corresponding author: e-mail: kzietarska@zut.edu.pl*

The study examined the adsorption of propan-1-ol (1PN) vapour on Sorbonorit 4 (S4) activated carbon in cyclic Electrothermal Temperature Swing Adsorption (ETSA) process. Dynamic adsorption capacity and breakthrough time were determined based on column studies. Thomas model was used to describe experimental breakthrough curves. Adsorption isotherms for 1PN vapour on S4 activated carbon were tested at 293 to 413 K. The experimental data were examined by using three multi-temperature isotherm models: Toth, Sips and hybrid Langmuir-Sips. Results indicate that S4 activated carbon is a heterogeneous adsorbent and the hybrid Langmuir-Sips model provides the best-fit experimental data. The energy requirement for 1PN electrothermal desorption from S4 bed (ca. 170–200 kJ/mol) was about 3 to 3.5 times larger than the isosteric heat of adsorption (56.8 kJ/mol), which was calculated using Toth adsorption isotherm.

Keywords: activated carbon, propan-1-ol, multi-temperature isotherms, electrothermal desorption, breakthrough curve.

INTRODUCTION

Propan-1-ol (1PN) is very flammable aliphatic alcohol which exhibits excellent dissolving, dispersing and degreasing properties. The substance is mainly used as a solvent in cosmetics, pharmaceutics (disinfectants), as well as cleaning/washing agents, paints, coating materials and printing inks. It may be released into the environment during a variety of chemical processes (*e.g.,* extraction, dissolving, mixing or filling) as well during processing to intermediates. 1PN vapour degrades in the atmosphere by reaction with photochemically-produced hydroxyl radicals, the half-life for this reaction being of 2.9 days[1].

Although a number of methods may be applied to reduce solvent vapour emission, Temperature Swing Adsorption (TSA) process is commonly used for waste gas purification[2, 3, 4]. It usually consists of two adsorbers with fixed bed activated carbon that are operated alternately in the adsorption and thermal regeneration modes. However, activated carbon adsorption capacity gradually depletes during the adsorption step which inhibits the purification efficiency. Once the permissible vapour concentration is reached in the purified gas, the spent adsorbent should be regenerated in situ. Typical TSA systems use thermal regeneration with steam or hot inert gas. One of the process variants is an Electrothermal Temperature Swing Adsorption (ETSA), where the activated carbon is regenerated by direct resistance heating method. The electrothermal method offers a real alternative to the conventional thermal methods[5].

To properly design an efficient carbon adsorption system, equilibrium and dynamic column tests should be performed. Based on them, the appropriate adsorbent and process operating conditions may be selected. The primary requirements for the adsorbents include: sufficient adsorption capacity in a wide range of adsorbate concentrations, appropriate selectivity, as well as mechanical, chemical and thermal stability[3].

In our earlier work[6], it was demonstrated that the efficiency of the 1PN vapour adsorption on S4 in ETSA system is the most effective for fully saturated adsorbent bed. It was concluded that the air purification should be performed in the co-flow ETSA system with several adsorption columns connected in series. This can ensure suitable regeneration efficiency and a long service life of the adsorbent.

The main objective of this study was to evaluate the effect of multiple electrothermal regeneration of adsorbent bed on the adsorption capacity. The analysis was performed based on the equilibrium and dynamic test results. Three multi-temperature isotherm and Thomas models were used to fit experimental data. On this basis, the adsorption capacity and characteristic parameters of the fixed-bed were determined. Moreover, the comparison between the energy demand for the desorption process and the isosteric heat of adsorption was presented.

EXPERIMENTAL SECTION

Material

Activated carbon Sorbonorit 4 (S4) was selected as an adsorbent. It was produced from peat by Norit Ltd. (The Netherlands). The adsorbent consisted of cylindrical pellets with diameter about 3.8 mm and length of 5 to 13 mm[7]. Considering its hardness and favourable adsorption properties, it can be used in solvent vapour removal processes.

Propan-1-ol (1PN) with analytical purity of 99.7% purchased from Chempur (Poland) was used as an adsorbate. The basic properties of 1PN are presented in Table 1. It is a clear, colourless liquid with a sharp musty odour similar to ethanol. The lowest explosive limit for 1PN is 2.1%. It is used in making cosmetics, skin and hair preparations, pharmaceuticals, perfumes, lacquer formulations, dye solutions, antifreezes, rubbing alcohols, soaps, windows cleaner and other cleaning products[9]. Owing to the excellent solubility in water and most organic liquids, it is used as intermediates or solvents[1].

Table 1. Physical and chemical properties of 1PN at 293 K[8]

Molecular formula	Molecular weight [g mol^{-1}]	Boiling point [K]	Saturation pressure [Pa]	Liquid molar volume [cm^3 mol^{-1}]	Enthalpy of vaporization [kJ mol^{-1}]
C_3H_8O	60.096	370.35	1993	74.939	41.38

Apparatus and procedure

Adsorption isotherm study

Adsorption isotherm measurements of 1PN vapour on S4 activated carbon were conducted using an intelligent gravimetric analyser IGA-002 (Hiden Isochema Ltd, UK). It is a precise microbalance system with a resolution of 0.1 μg and an uncertainty of ± 1 μg. A sample of activated carbon with a mass of *ca.* 86 mg was placed in the thermostated reactor chamber with accurate temperature control (± 0.1 K). Before the isotherm measurements, the S4 was outgassed to a constant weight at high vacuum level (10^{-6} Pa) at 393 K for 2 hours. The measurements were conducted at 293, 313, 333, 348, 373, 393 and 413 K and pressure of up to 2430 Pa. The equilibrium points were collected and plotted as an isotherm. The adsorption capacity was calculated for all of the isotherms as the ratio between adsorbed 1PN and the mass of adsorbent sample after degassing. A comprehensive description of the methodology of isotherm determination with IGA-002 is presented elsewhere[10].

Dynamic adsorption tests

Dynamic adsorption studies were conducted in a laboratory-scale ETSA setup consisting of vapour generation device, adsorber, resistance heating device, a data acquisition and control system. A glass column (0.055 m internal diameter) with S4 fixed-bed with the mass of 0.26 kg and height of 0.27 m was utilized as the adsorber.

The column was thermally insulated with mineral wool of 0.04 m width, for reducing the heat loss with surroundings. A comprehensive description of the experimental setup can be found elsewhere[11].

The ETSA cycle consisted of adsorption, electrothermal desorption and cooling steps. During the adsorption step the dynamic tests were performed. All experiments were performed at ambient temperature (295 $\pm$3K) under the following operating conditions: inlet concentration of 1PN vapour C_0 = 6–9 g/m^3, gas flow rate Q = 2.15 m^3/hr (superficial gas velocity 0.24 m/s). The experiments were conducted until the exhaust stream reached a particular breakthrough concentration. Some of adsorption cycles were conducted until the bed reached saturation, indicated by a stable concentration at the column outlet. After the completion of all tests, the saturated adsorbent was regenerated by using the direct resistive heating method. The electrothermal desorption experiments were performed in the following invariability range of parameters: 30 V voltage, 0.08–0.22 m^3/hr nitrogen flow and 403–413 K temperature. The results of the 1PN desorption step were detailed elsewhere[6].

RESULT AND DISCUSSION

Column studies

Dynamic adsorption results are shown as S-shaped time-concentration profiles of 1PN-S4 system at the column outlet. The curves commonly called breakthrough curves, describe the relationship between the outlet-to-inlet 1PN vapour concentration (C/C_0) and adsorption time.

Figure 1 presents several experimental breakthrough curves for adsorption subsequent cycles of ETSA process. In P1 cycle, the adsorption was conducted using a fresh adsorbent. Activated carbon regenerated with direct resistive method was used in other cycles.

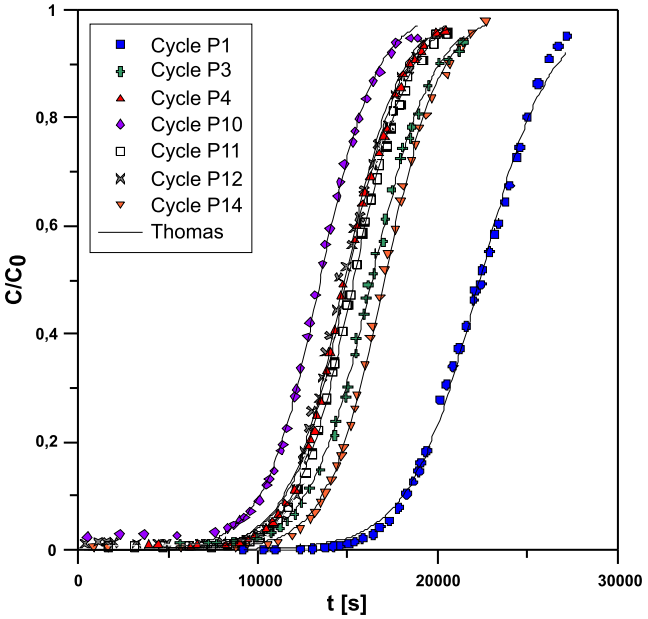

Figure 1. Breakthrough curves for 1PN adsorption in ETSA process, at constans superficial gas velocity

As can be seen, the breakthrough curves for the same inlet adsorbate concentration (ca. 8.5 g/m^3) were almost overlapped, therefore it may be assumed that the steady state for fixed-bed was reached after the third cycle. In a cyclic adsorption process, an adsorbent service life depends on adsorption process conditions (temperature, inlet concentration, gas flow velocity) and the degree of activated carbon regeneration[3]. Too low adsorbent regeneration efficiency in a given ETSA cycle lowers adsorption duration in a successive cycle, as evidenced by shifted breakthrough curves in Figure 1. The breakthrough curves were predicted using the Thomas model[12, 13] described by Eq. (1), where K_{Th} is Thomas rate constant (m^3/(kg · s)), Q the volumetric flow rate (m^3/s), q_{sat} the saturation capacity (kg/kg), m_{ads} the adsorbent mass (kg) and t the adsorption time (s).

$$\frac{C}{C_0} = \frac{1}{1 + \exp\left(\frac{K_{Th} q_{sat} m_{ads}}{Q} - C_0 K_{Th} t\right)} \tag{1}$$

The Thomas model assumes plug-flow behaviour and neglects axial dispersion. It employs the Langmuir isotherm and pseudo second-order kinetic model. The model is suitable for gas adsorption process with a constant flow rate. Model parameters, which were determined with nonlinear regression method using Statistica 12.5 software, are summarized in Table 2.

Table 2. The breakthrough curve parameters for 1PN vapour adsorption process at 298 K

Cycle number	C_0 [g m^{-3}]	$t_{5\%}$ [s]	q_{re} [kg kg^{-1}]	q_{exp} [kg kg^{-1}]	K_{th} [m^{3}kgs^{-1}]	q_{sat} [kg kg^{-1}]	R^2 [–]
P1	6.545	17130	0	0.3287	0.0788	0.3202	0.9985
P3	7.614	11577	0.0503	0.2788	0.0775	0.2806	0.9995
P4	8.396	10571	0.0530	0.2942	0.0767	0.2887	0.9995
P5	8.529	10877	0.0696	0.3006	0.0740	0.3001	0.9995
P6	8.448	10123	0.0526	0.2861	0.0717	0.2921	0.9995
P7	8.531	10281	0.0540	0.2867	0.0751	0.2901	0.9995
P8	8.877	10927	0.0477	0.2948	0.0703	0.3090	0.9992
P10	8.580	8866	0.0106	0.2614	0.0753	0.2655	0.9991
P11	8.809	11090	0.0693	0.3120	0.0732	0.3104	0.9997
P12	8.693	10926	0.0571	0.2944	0.0758	0.2965	0.9980
P13	8.590	10658	0.0406	0.2954	0.0731	0.3003	0.9994
P14	8.460	12774	0.0815	0.3312	0.0752	0.3312	0.9997

Calculated theoretical breakthrough curves were consistent with the corresponding experimental data (Fig. 1), as evidenced by the values of determination coefficient, *i.e.*, $R^2 > 0.998$.

Breakthrough curves were analysed by determining the following parameters: the breakthrough time ($t_{5\%}$), which is defined as the time when outlet relative concentration equals 5% of 1PN inlet concentration[14], the adsorbent capacity, which is the amount of adsorbate retained on the surface of the adsorbent divided by the mass of the adsorbent bed. Adsorption capacity can be determined depending on the area above the breakthrough curve at the column outlet[15,16] using Eq. (2), where q_{C/C_0} (kg/kg) is the capacity of fixed-bed at the time t_{C/C_0} (s), m_{ads} (kg) the adsorbent mass, V the fluid flow rate (m^3/s), C_0 and C are the inlet and outlet concentration (kg/m^3).

$$q_{C/C_0} = \frac{VC_0}{m_{ads}} \int_0^{t_{C/C_0}} \left(1 - \frac{C}{C_0}\right) dt \tag{2}$$

Table 2 shows that the working adsorption capacity (q_{exp}) determined at $C/C_0 = 0.95$ depends on input vapour concentration and the efficiency of the adsorbent regeneration in preceding cycle. In the case of full regeneration, the adsorption capacity is identical to that of the first cycle of ETSA (residual loading $q_{res} = 0$). This condition is not fulfilled for the analysed cycles, as evidenced by the values of residual loading shown in Table 2. When the efficiency of regeneration is lower, the value of residual loading is lower too. Consequently, the lifetime of the bed is shorter in subsequent cycle.

A comparison of q_{exp} and q_{sat} adsorption capacities (Table 2) for the same inlet concentration, which were determined by Eq. (1) and (2), shows that the Thomas model provides quite good fit for all presented cycles. Table 2 shows that q_{th} estimated by Thomas model is very close to the working adsorption capacity q_{exp} obtained experimentally.

Adsorption isotherms

Multi-temperature isotherm models

The multi-temperature isotherm models, that are provided to predict the adsorption capacity at any temperature and concentration, are very useful for proper design and simulation of ETSA processes. Three different models, *i.e.*, Toth, Sips and hybrid Langmuir-Sips, were employed to describe the experimental equilibrium data.

The Toth model is an empirical expression used to describe a monolayer adsorption and it can be applied to Type I isotherms. It is valid in the whole range of the vapour pressure. It assumes adsorption on energetically heterogeneous surface with most sites having adsorption energy lower than the maximum. The Toth model is given by Eq. (3)[17], where q (mol/kg), is the adsorption capacity, q_{mT} (mol/kg) the maximum adsorption capacity, p (Pa) the equilibrium pressure of the adsorbate, b_{0T} (Pa^{n_T}) and n_T are the parameters of the equation which are linked by Eq. (4). Other parameters in Eq. (4) are as follows: T (K) is the temperature, ΔH (J/mol) the heat of adsorption, $R = 8.314$ J/(mol · K) the universal gas constant and b_{0T} (Pa^{n_T}) the pre-exponential factor.

$$q = q_{mT} \frac{p}{\left(b_T + p^{n_T}\right)^{1/n_T}} \tag{3}$$

$$b_T = b_{0T} \exp\left(-\frac{n_T \cdot \Delta H}{R \cdot T}\right) \tag{4}$$

The second empirical model is the Sips model given by Eq. (5)[15, 16]. Its characteristic parameters, *i.e.*, q_{mS} (mol/kg), b_S (Pa^{-1}) and n_S, are expressed depending on the absolute temperature (T) using Eqs. (6)–(8), where q_{0S} (mol/kg), q_{1S}, b_{0S} (Pa^{-1}), Q_S (J/mol), n_{0S} and n_{1S} are the parameters of the equations and $T_0 = 293$ K is the reference temperature. The Sips model is a combination of Langmuir and Freundlich isotherms. At low adsorbate concentration, this model reduces the form to Freundlich isotherm and thus does not follow the Henry's law. At high concentrations, it predicts a monolayer adsorption capacity characteristic of the Langmuir isotherm.

$$q = q_{mS} \frac{\left(b_S \cdot p\right)^{n_S}}{1 + \left(b_S \cdot p\right)^{n_S}} \tag{5}$$

$$q_{mS} = q_{0S} \cdot \exp\left(q_{1S} \cdot \left(1 - \frac{T}{T_0}\right)\right) \tag{6}$$

$$b_S = b_{0S} \cdot \exp\left(\frac{Q_S}{RT_0} \cdot \left(\frac{T_0}{T} - 1\right)\right) \tag{7}$$

$$n_S = n_{0S} + n_{1S} \cdot \left(1 - \frac{T_0}{T}\right) \tag{8}$$

The hybrid Langmuir-Sips model was developed for the adsorptions-condensation of vapours on porous adsorbents. It consist of two separate regions: the former is linear or favourable and depends on the Langmuir isotherm parameter and the latter depends on the Sips isotherm parameter and greatly affects the capillary

condensation region[18]. The hybrid model is described by Eq. (9)[18] and its characteristic parameters, *i.e.*, q_{mLS} (mol/kg), b_{1LS} (Pa^{-1}), b_{2LS} ($Pa^{-n_{LS}}$) and n_{LS}, are given by Eqs. (10)–(13) depending on q_{0LS} (mol/kg), q_{1LS} (J/mol), b_{01LS} (Pa^{-1}), Q_{1LS} (J/mol), b_{02LS} ($Pa^{-n_{LS}}$), Q_{2LS} (J/mol), n_{0LS} and n_{1LS} (J/mol).

$$q = q_{mLS} \cdot \left[\frac{b_{1LS} \cdot p}{1 + b_{1LS} \cdot p} + \frac{b_{2LS} \cdot p^{n_{LS}}}{1 + b_{2LS} \cdot p^{n_{LS}}} \right] \tag{9}$$

$$q_{mLS} = q_{0LS} \cdot \exp\left(\frac{q_{1LS}}{R} \cdot \left(\frac{1}{T} - \frac{1}{T_0} \right) \right) \tag{10}$$

$$b_{1LS} = b_{01LS} \cdot \left(-\frac{Q_{1LS}}{R} \cdot \left(\frac{1}{T} - \frac{1}{T_0} \right) \right) \tag{11}$$

$$b_{2LS} = b_{02LS} \cdot \left(-\frac{Q_{2LS}}{R} \cdot \left(\frac{1}{T} - \frac{1}{T_0} \right) \right) \tag{12}$$

$$n_{LS} = n_{0LS} \cdot \left(-\frac{n_{1LS}}{R} \cdot \left(\frac{1}{T} - \frac{1}{T_0} \right) \right) \tag{13}$$

Modelling of experimental equilibrium data

Table 3 presents the isotherm equation parameters determined with the nonlinear regression method. They were determined with the Levenberg-Marquardt method using Statistica 12.5 software. The average relative error (ARE)[10] was used to evaluate model fit do data, expressed by Eq. (14), where q_{expi} is the experimental adsorption capacity, q_{calci} the calculated adsorption capacity and N the number of experimental points.

$$ARE = \frac{100}{N} \cdot \sum_{i=1}^{N} \left| \frac{q_{\exp i} - q_{cal\,i}}{q_{\exp i}} \right| \tag{14}$$

As indicated by the ARE values in Table 3 for 1PN-S4 system, the hybrid Langmuir-Sips model given a better fitting of the equilibrium data (ARE = 2.70%), than the two other models (ARE = 7.6% and ARE = 11.95%).

Figure 2, which presents the experimental and simulated adsorption isotherms of 1PN on S4 activated carbon, shows that all simulated isotherm curves agree well with the experimental results. It can be also observed that the adsorbate amount decreased with an increase in the temperature. This is indicative of a physical adsorption. The adsorption isotherms are classified as Type I (IUPAC classification). However, in high-pressure range, the isotherm at 293 K shows some deviations from monolayer adsorption. This phenomenon is typical for adsorbents with a large porosity. The data analysis revealed that the working adsorption capacities determined from the breakthrough experiments were within 80–95% of the estimated maximum adsorption capacity from the Toth isotherm (0.348 kg/kg).

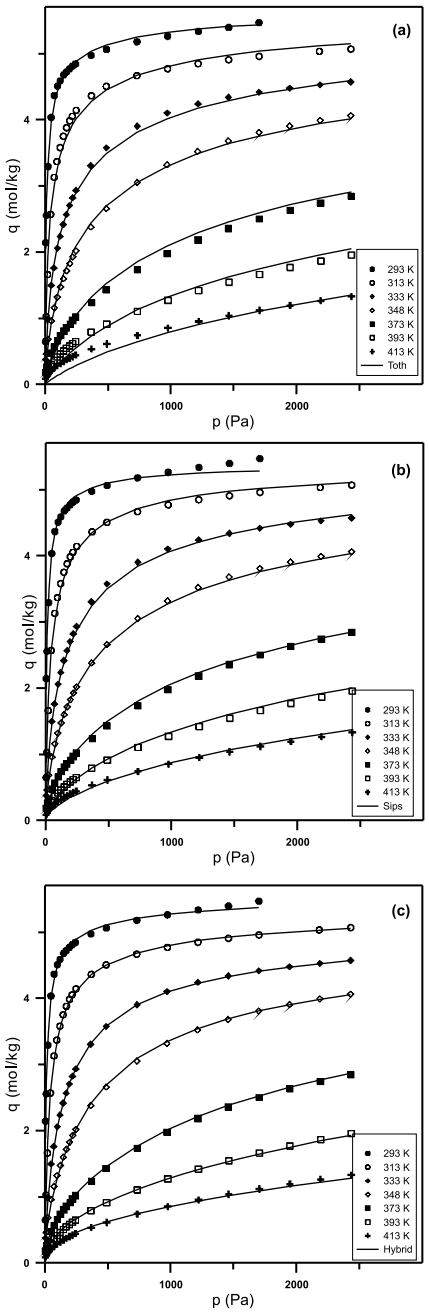

Figure 2. Experimental adsorption isotherms of 1PN vapours on Sorbonorit 4 at various temperatures; experimental data (points) and fitted curve by: (a) Toth model, (b) Sips model, (c) Hybrid Langmuir-Sips model

Table 3. Parameters and errors of multi – temperature adsorption isotherms

Toth Model		SIPS Model		Hybrid Model	
q_m [mol kg^{-1}]	5.79182	q_{0S} [mol kg^{-1}]	5.53702	q_{0LS} [mol kg^{-1}]	2.81747
b_{0T} [$Pa \cdot n_T^{-1}$]	632738.12	q_{1S} [–]	0.04929	q_{1LS} [J/mol^{-1}]	1057455.08
n_t [–]	0.52932	T_0 [K]	293.15	b_{01LS} [Pa^{-1}]	0.13639
ΔH [J mol^{-1}]	58925.32	b_{0S} [Pa^{-1}]	0.08431	Q_{1LS} [J mol^{-1}]	63274.31
ARE [%]	11.94564	n_{0S} [–]	24.08478	b_{02LS} [$Pa \cdot n_{LS}^{-1}$]	0.12713
R^2 [–]	0.9984	n_{1S} [–]	0.67483	Q_{2LS} [J mol^{-1}]	17264.02
		Q_S [J mol^{-1}]	58700.59	n_{0LS} [–]	0.58736
		ARE [%]	7.61342	n_{1LS} [J mol^{-1}]	2101.03
		R^2 [–]	0.9992	*ARE* [%]	2.69597
				R^2 [–]	0.9981

Isosteric heat of adsorption

The isosteric heat of adsorption corresponds to the energy released in the fixed-bed during the adsorption process. It characterizes the strength of adsorbate-adsorbent and adsorbate-adsorbate interactions, as well as the nature of adsorbents surface. Figure 3 presents the dependence of isosteric heat value on the adsorbate amount. The isosteric heat of adsorption, Q_{st} (J/mol), was calculated depending on multi-temperature adsorption isotherm using Clausius-Clapeyron equation (15)[15], where R = 8.314 J/(mol · K) is the universal gas constant, T (K) the temperature and p (Pa) the pressure.

$$Q_{st} = -R \cdot \left(\frac{\partial \ln p}{\partial \left(\frac{1}{T} \right)} \right)_q \tag{15}$$

The point and dotted plots represent the isosteric heat of adsorption calculated using Clausius-Clapeyron (15) and Toth (3) equations, respectively. According to Toth model, the heat of adsorption should be independent of coverage. As can be seen from Figure 3, the Q_{st} varies with increasing of the adsorbate loading q. It is the effect of the S4 surface heterogeneity, which was confirmed by results of X-ray photoelectron spectroscopy analysis presented elsewhere[11].

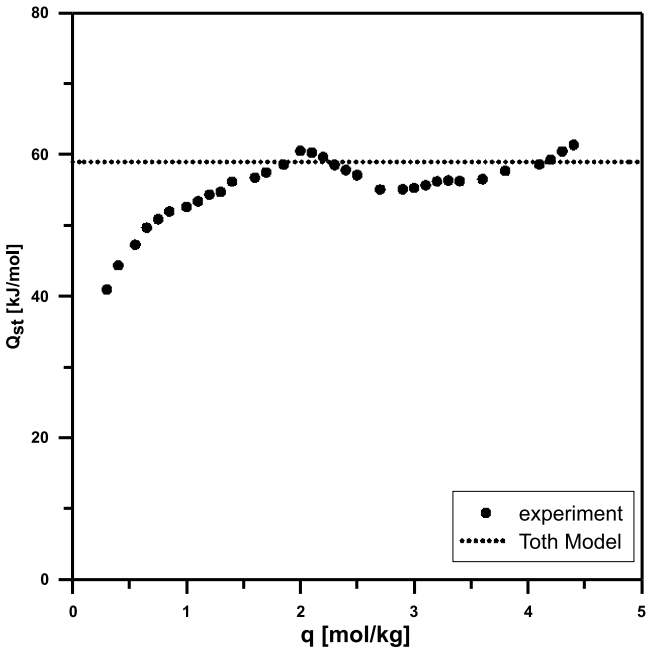

Figure 3. The isosteric heat of adsorption of 1PN on Sorbonorit 4

Figure 3 shows that the isosteric heat of adsorption for 1PN increases from about 40 kJ/mol to 60 kJ/mol and then decrease by 5 kJ/mol). Its value is almost constant in the loading range of 2.2 to 3.6 mol/kg. At high coverage, the heat value rises to 62 kJ/mol. The plot suggests that the various interactions may be responsible for a complex adsorption behaviour. A similar relationship between the Q_{st} and q values was observed for propanol isomers vapours adsorption on Sorbonorit B4 activated carbon. More details in this regard can be found elsewhere[18]. The initial increase in the isosteric heat of adsorption with an increase in adsorbate loading indicates that intermolecular interactions between the 1PN molecules are dominant over adsorbate-adsorbent interactions[20, 21]. As can be seen, the Toth isotherm model yields overestimated average value of Q_{st} (ΔH = 56.8 kJ/mol) in comparison to experimental results. However, in the adsorbent loading range of 1.1 to 4.3 mol/kg, the difference between the values of Q_{st} is up to 6%. The value of isosteric calculate using the Toth equation is 1.4 times larger than its heat of vaporization (ΔH_{vap} = 41.38 kJ/mol), which is typical for physical adsorption. It is generally assumed that Q_{st} represents the minimum energy needed to desorb an adsorbate. However, in our earlier works[6], the total energy demand for 1PN desorption was about 170–200 kJ/mol, which is roughly 3–3.5 times larger than the Qst value. This indicates that a significant amount of the total energy was used to heat the adsorbate, adsorbent bed, carrier gas and installation equipment (column, pipes, connectors) and was lost to the surrounding[5, 22].

CONCLUSIONS

In this paper, equilibrium and dynamic adsorption tests were used to the evaluation of 1PN vapour adsorption performance of the Sorbonorit 4 activated carbon. The adsorption equilibrium measurements at different temperatures (293 to 413 K) and 1PN vapour pressures were carried out. The isotherm modelling demonstrated that S4 is a heterogeneous adsorbent and that the hybrid Langmuir-Sips equation provided a good agreement with experimental data (ARE = 2.7%).

Dynamic adsorption tests in ETSA system highlighted that the adsorption efficiency of 1PN vapour on Sorbonorit 4 was dependent on adsorbate input concentration and the degree of adsorbent regeneration in a preceding adsorption cycle. Improperly selected operation parameters of electrothermal desorption led to a shortened service life of a bed at the adsorption step in a successive ETSA cycle. The Thomas model provided a good fit of experimental breakthrough curves for 1PN vapour on S4.

LITERATURE CITED

1. European Union Risk Assessment Report: Propan-1-ol. Vol. 82, Part I – Environment. (2017, April) https://echa.europa.eu/documents/10162/3fd81f2f-b48d-4123-88ea-12e88b53850f

2. Moretti, E.C. (2002). Reduce VOC and HAP emissions. Chem. Eng. Prog. 98, 6, 30–40.

3. Bathen, D. & Breitbach, M. (2001). Adsorptionstechnik. Springer-Verlag, Berlin-Heidelberg.

4. Sharma, P.K. & Wankat, P.C. (2010). Solvent recovery by steamless Temperature Swing Carbon Adsorption processes. Ind. Eng. Chem. Res. 49, 11602–11613. DOI: 10.1021/ie1008019.

5. Downarowicz, D. & Gabruś, E. (2008). Electrothermal Temperature Swing Adsorption. A chance of effective VOC recovery from flue gases. Przem. Chem. 87, 768–774.

6. Downarowicz, D. & Gabruś E. (2010). Air purification from 1-propanol vapours in ETSA process. Air Protection in Theory and Practice, Institute of Environmental Engineering Polish Academy of Sciences in Zabrze. ISBN 978-83-60877-48-7.

7. Gu, J., Faqir, N.M. & Bart, H.J. (1999). Drying of an activated carbon column after steam regeneration. Chem. Eng. Technol. 22, 859–864.

8. Yaws, C.L. (2003). Yaws' Handbook of thermodynamic and physical properties of chemical compounds. Knovel, New York.

9. PubChem, Open Chemistry Data base (2017, April). https://pubchem.ncbi.nlm.nih.gov/compound/1-propanol#section=Top

10. Nastaj, J. & Aleksandrzak, T. (2013). Adsorption isotherms of water, propan-2-ol, and methylbenzene vapors on Grade 03 silica gel, Sorbonorit 4 activated carbon, and Hisiv3000 zeolite. J. Chem. Eng. Data 58, 2629–2641. DOI: 10.1021/je400517c.

11. Downarowicz, D. (2015). Adsorption characteristics of propan-2-ol vapours on activated carbon Sorbonorit 4 in electrothermal temperature swing adsorption process. Adsorption 21, 87–98. DOI: 10.1007/s10450-015-9652-1.

12. Calero, M., Hernáinz, F., Blázquez, G., Tenorio, G. & Martín-Lara, M.A. (2009). Study of Cr (III) biosorption in a fixed-bed column. J. Hazard. Mater. 171, 886–893. DOI: 10.1016/j.jhazmat.2009.06.082.

13. Srivastava, V.C., Prasad, B., Mishra, I.M., Mall, I.D. & Swamy, M.M. (2008). Prediction of breakthrough curves for sorptive removal of phenol by bagasse fly ash packed bed. Ind. Eng. Chem. Res. 47, 1603–1613. DOI: 10.1021/ie0708475.

14. Namane, A. & Hellal, A. (2006). The dynamic adsorption characteristics of phenol by granular activated carbon. J. Hazard. Mater. B137, 618–625. DOI: 10.1016/j.jhazmat.2006.02.052.

15. Gabruś, E. & Downarowicz, D. (2016). Anhydrous ethanol recovery from wet air in TSA systems - equilibrium and column studies. Chem. Eng. J. 288, 321–331. DOI: 10.1016/j.cej.2015.11.110.

16. Duong, D. Do, Adsorption Analysis: Equilibria and Kinetics, Imperial College Press 1998, ISBN 1-86094-130-3.

17. Taqvi, S.M., Appel, W.S. & LeVan, M.D. (1999). Coadsorption of organic compounds and water vapour on BPL activated carbon. 4. methanol, ethanol, propanol, butanol, and modelling. Ind. Eng. Chem. Res. 38, 240–250. DOI: 10.1021/ie980324k.

18. Lee, J.W., Shim, W.G., Yang, M.S. & Moon, H. (2004). Adsorption isotherms of polar and nonpolar organic compounds on MCM-48 at (303.15, 313.15, and 323.15) K. J. Chem. Eng. Data. 49, 502–509. DOI: 10.1021/je030208a.

19. Downarowicz, D. & Aleksandrzak, T. (2016). Adsorption of popanol isomer vapors on Sorbonorit B4 activated carbon: Equilibrium and spectroscopic studies, J. Chem. Eng. Data. 61, 3652–365. DOI: 10.1021/acs.jced.6b00583.

20. Andreu, H.F. Stoeckli, R.H. Bradley. (2007). Specific and non-specific interactions on non-porous carbon black surfaces. Carbon 45, 1854–1864. DOI: 10.1016/j.carbon.2007.04.025.

21. Tolmachev, A.M., Firsov, D.A., Anuchin, K.M. & Fomkin A.A. (2008). Simulating of Alcohol Adsorption in Slitlike Micropores of Active Carbon by the Molecular Dynamics Method. Coll. J. 70, 486–496. DOI: 10.1134/S1061933X08040133.

22. Dombrowski, K.D., Lehmann, C.M., Sullivan, P.D., Ramirez, D., Rood, M.J. & Hay, K.J. (2004). Organic vapor recovery and energy efficiency during electric regeneration of an activated carbon fiber cloth adsorber. J. Environ. Eng. 130(3), 268–275. DOI: 10.1061/(ASCE)0733-9372(2004)130:3(268).